

Level densities and γ -ray strength functions in $^{170,171,172}\text{Yb}$

U. Agvaanluvsan,^{1*} A. Schiller,² J. A. Becker,² L. A. Bernstein,² P. E. Garrett,² M. Guttormsen,³ G. E. Mitchell,^{1,4}
J. Rekestad,³ S. Siem,³ A. Voinov⁵, and W. Younes²

¹*Department of Physics, North Carolina State University, Raleigh, NC 27695, USA*

²*Lawrence Livermore National Laboratory, L-414, 7000 East Avenue, Livermore, CA 94551, USA*

³*Department of Physics, University of Oslo, N-0316 Oslo, Norway*

⁴*Triangle Universities Nuclear Laboratory, Durham, NC 27708, USA*

⁵*Department of Physics, Ohio University, Athens, OH 45701, USA*

Level densities and radiative strength functions in ^{171}Yb and ^{170}Yb nuclei have been measured using the $^{171}\text{Yb}(^3\text{He}, ^3\text{He}'\gamma)^{171}\text{Yb}$ and $^{171}\text{Yb}(^3\text{He}, \alpha\gamma)^{170}\text{Yb}$ reactions. New data on ^{171}Yb are compared to a previous measurement for ^{171}Yb from the $^{172}\text{Yb}(^3\text{He}, \alpha\gamma)^{171}\text{Yb}$ reaction. Systematics of level densities and radiative strength functions in $^{170,171,172}\text{Yb}$ are established. The entropy excess in ^{171}Yb relative to the even-even nuclei $^{170,172}\text{Yb}$ due to the unpaired neutron quasiparticle is found to be approximately $2k_B$. Results for the radiative strength function from the two reactions lead to consistent parameters characterizing the “pygmy” resonances. Pygmy resonances in the $^{170,172}\text{Yb}$ populated by the $(^3\text{He}, \alpha)$ reaction appear to be split into two components for both of which a complete set of resonance parameters are obtained.

PACS number(s): 21.10.Ma, 24.30.Gd, 25.55.Hp, 27.70.+q

I. INTRODUCTION

Nuclear level densities and radiative strength functions are important inputs for calculations of nuclear reaction cross sections. In addition to their value in practical applications, these average quantities may shed light on the understanding of such fundamental issues as the transition from the discrete (low excitation) to statistical (high excitation) regime. At low excitation energy, the level density is obtained directly by counting low-lying levels. However, at increasing excitation energy, the level density becomes large and individual levels are often not resolved in experiments [1]. Nuclear resonances at or above the nucleon binding energy provide another source of level density data [2]. Between these two excitation energy regions, relatively little is known about nuclear level densities. The present paper focuses on this intermediate region.

A major part of the information on radiative strength functions comes from photoabsorption cross section measurements [3]. High energy γ transitions ($E_\gamma \sim 10 - 15$ MeV) are dominated by the giant electric dipole resonance (GEDR). Although the electric dipole transition strengths are well studied in the vicinity of the GEDR, the behavior of low energy γ rays is less well understood [4]. This is particularly true for radiative transitions between highly excited states. Experimental data on the $M1$ strength function are much scarcer than for the $E1$ strength function. In these regions, an experimental technique recently developed by the Oslo Cyclotron Group provides valuable data. This method allows one to de-

termine level densities and radiative strength functions simultaneously [5,6] from the primary γ -ray spectra. The advantage of this method is that it provides data on nuclear level densities and radiative strength functions in regions where there is little information and data is difficult to obtain. However, the level density and radiative strength function are coupled, since the γ decay input to the technique depends on both quantities. A shortcoming of the method is that the absolute level density and radiative strength function need to be normalized using the low-lying discrete states, neutron resonance spacings, and average total radiative widths of neutron resonances. Thus the primary new contribution is the energy dependence of the level density and the radiative strength function. This method is commonly referred to as the Oslo method. It has been shown to work well in heavy-mass nuclei and has been extended to other mass regions as well [7,8]. The present paper reports new results from a $^{171}\text{Yb} + ^3\text{He}$ experiment. The Oslo method and the experimental set-up are briefly discussed, followed by a brief description of level densities and radiative strength functions. The results for ^{171}Yb obtained from two different reactions, $^{171}\text{Yb}(^3\text{He}, ^3\text{He}')^{171}\text{Yb}$ and $^{172}\text{Yb}(^3\text{He}, \alpha)^{171}\text{Yb}$, are compared. The similar comparison for ^{172}Yb , previously reported, is repeated for the sake of completeness.

II. EXPERIMENTAL METHODS

The experiment was conducted at the Oslo Cyclotron Laboratory (OCL) using a 45-MeV ^3He beam. The self-

*Electronic address: agvaanluvsan1@llnl.gov

supporting targets of $^{171,172,173}\text{Yb}$ enriched to $\sim 95\%$ had a thickness of $\sim 2\text{ mg cm}^{-2}$. Five reactions studied in this paper are:

- 1) $^{171}\text{Yb}(^3\text{He},\alpha)^{170}\text{Yb}$ (new)
- 2) $^{171}\text{Yb}(^3\text{He},^3\text{He}')^{171}\text{Yb}$ (new)
- 3) $^{172}\text{Yb}(^3\text{He},\alpha)^{171}\text{Yb}$ (reported previously in [9,10])
- 4) $^{172}\text{Yb}(^3\text{He},^3\text{He}')^{172}\text{Yb}$ (reported previously in [11])
- 5) $^{173}\text{Yb}(^3\text{He},\alpha)^{172}\text{Yb}$ (reported previously in [9,10]).

Particle- γ coincidences for $^{170,171,172}\text{Yb}$ were detected using the CACTUS multidetector array [12]. The charged particles were measured with eight Si particle telescopes placed at 45° with respect to the beam direction. Each telescope consists of a front Si ΔE detector and a back Si(Li) E detector with thicknesses 140 and 3000 μm , respectively. An array of 28 collimated NaI γ -ray detectors with a total coverage of $\sim 15\%$ of 4π surrounds the target. In addition one to three Ge detectors were used to estimate the spin distribution and determine the selectivity of the reaction. The typical spin range is expected to be $I \sim 2 - 6\hbar$. Experiments run for ~ 2 weeks with typical beam currents of $\sim 1.5\text{ nA}$.

The data analysis consists of three main steps. The first step is to prepare the particle- γ coincidence matrix. For each particle energy bin total cascade γ -ray spectra are obtained from the coincidence measurement. The particle energy is transformed to excitation energy using the reaction kinematics. Then each row of the coincidence matrix corresponds to a certain excitation energy E_x in the residual nucleus, while each column corresponds to a certain γ -ray energy E_γ . The second step is the unfolding. The γ -ray spectrum is unfolded using the known response function of the CACTUS array [13]. The γ -ray spectrum containing only the first γ rays emitted from a given excitation energy is called the first-generation spectrum and denoted by P . The matrix which consists of first generation spectra is obtained in the third step for each excitation energy bin using the subtraction procedure described in Ref. [14]. The key assumption of this method is that the γ decay from any excitation energy bin is independent of the method of formation, either directly by the nuclear reaction or by γ decay from higher lying states following the initial reaction. This assumption is automatically fulfilled when the same states are populated equally via the two processes, since γ branching ratios are properties of levels. Even if different states are populated, the assumption is still valid for statistical γ decay, which depends only on the γ -ray energy and the number of available final states. These assumptions have been investigated extensively over the years by the Oslo group and shown to work reasonably well [6]. The entries of the first generation matrix P are the probabilities $P(E_x, E_\gamma)$ that a γ -ray of energy E_γ is emitted from excitation energy E_x .

The probability of γ decay is proportional to the product of the γ -ray strength (i.e., the radiative transmission coefficient $\mathcal{T}(E_\gamma)$) and the level density $\rho(E_x - E_\gamma)$ at the final energy $E_x - E_\gamma$

$$P(E_x, E_\gamma) \propto \mathcal{T}(E_\gamma)\rho(E_x - E_\gamma). \quad (1)$$

This factorization is the generalized form of the Brink-Axel hypothesis [15,16] which states that the GEDR and any other excitation modes built on an excited state have the same properties as those built on the ground state. In other words, the radiative transition strength is independent of the excitation energy. There is evidence that the width of the giant-dipole resonance increases with increasing nuclear temperature of the state upon which it is built, and thus with its excitation energy $E_f = E_x - E_\gamma$ [17,18]. The temperature that corresponds to the excitation energy region covered in this work is rather low and changes slowly with excitation energy ($T \sim \sqrt{E_f}$). In this work we assume constant temperature and that the radiative strength function does not depend on the excitation energy in the energy interval under consideration.

In the Oslo method the functions ρ and \mathcal{T} are determined by an iterative procedure [5]. The goal of the iteration is to determine these two functions at $\sim N$ energy values each; the product of the two functions is known at $\sim N^2/2$ data points. The globalized fitting to the data points determines the functional form for ρ and \mathcal{T} [5]. However, it can be shown that the entries of matrix P in Eq. (1) given by the product of ρ and \mathcal{T} are invariant under the transformation [5]

$$\tilde{\rho}(E_x - E_\gamma) = A \exp[\alpha(E_x - E_\gamma)] \rho(E_x - E_\gamma), \quad (2)$$

$$\tilde{\mathcal{T}}(E_\gamma) = B \exp(\alpha E_\gamma) \mathcal{T}(E_\gamma). \quad (3)$$

Thus, in a final step, the transformation parameters A , B , and α , which correspond to the physical solution have to be determined. The level density ρ is determined from the nuclear ground state up to $\sim B_n - 1\text{ MeV}$, where B_n is the neutron binding energy. The coefficients A and α are determined from the normalization of the level density to data from the discrete levels and the neutron resonance spacings. The radiative transmission coefficient \mathcal{T} is obtained from $E_\gamma \approx 1\text{ MeV}$ to around B_n . The remaining constant B is determined from the normalization of the transmission coefficient to data from the total radiative widths of neutron resonances. The details of the normalization and consideration of the experimental results are discussed in the following sections.

III. LEVEL DENSITIES

The level density obtained from the present experiment covers the excitation energy from the ground state up to $\sim B_n - 1\text{ MeV}$. However, as described in the previous section, the level density must be normalized. Figure 1 illustrates the normalization procedure. The filled circles are our experimental data points for the reaction $^{171}\text{Yb}(^3\text{He},\alpha)^{170}\text{Yb}$. In the upper panel, the level density at low excitation energy determined from the present experimental data is compared to the histogram calculated using discrete levels listed in the Table of Isotopes [19].

The agreement is good up to $E_x \sim 1.6$ MeV. Above this energy the two results differ because there is limited information on discrete levels at higher excitation energy. Thus, the present experiment provides new results for the average level density above $E_x = 1.6$ MeV. Comparison at low excitation energy is used to fix the absolute value of the data at the low-energy end. In the lower panel, the normalization with respect to the neutron resonance spacing data is shown. The level density at B_n is determined using the neutron resonance spacing data [20]. Since our data only extend to ~ 1 MeV below B_n , an interpolation is required between the present experimental data and ρ evaluated at B_n . The back-shifted Fermi gas level density parameterized by von Egidy *et al.* [2],

$$\rho(E_x) = \eta \frac{\exp(2\sqrt{aU})}{12\sqrt{2}a^{1/4}U^{5/4}\sigma_I}, \quad (4)$$

is employed for the interpolation. The back-shifted excitation energy is given by $U = E_x - C_1 - \Delta$ where $C_1 = -6.6A^{-0.32}$ MeV, $a = 0.21 A^{0.87}$ MeV⁻¹ and the pairing parameter Δ is estimated following the prescription by Dobaczewski *et al.* [21]. For ¹⁷²Yb, a slightly different normalization was used. The level density for ¹⁷⁰Yb is about an order of magnitude smaller than the level density for ¹⁷¹Yb.

We report new results for the level density and radiative strength function obtained from reactions on the target nucleus ¹⁷¹Yb. For ¹⁷¹Yb, the level density and radiative strength function were obtained by two different reactions, one from the ¹⁷¹Yb(³He,³He' γ)¹⁷¹Yb reaction and another from the ¹⁷²Yb(³He, $\alpha\gamma$)¹⁷¹Yb reaction. The results from the ¹⁷²Yb(³He, $\alpha\gamma$)¹⁷¹Yb experiment were reported previously in [9,10]. Similarly, the level density in ¹⁷²Yb is obtained by two reactions.

Figure 2 shows the level densities of ^{170,171,172}Yb from the ground state up to $\sim B_n - 1$ MeV. Data points shown in full circles are from the (³He, $\alpha\gamma$) reaction and in open circles from the (³He,³He' γ) reaction. The effect which yields an overestimated level density at low excitation ~ 0.5 MeV from (³He,³He') reaction data is due to a disproportional population of states with relatively large transition matrix elements to the ground state rotational band. More details on this effect are given in Ref. [22]. Except for this effect, the agreement between level densities for the same nucleus obtained via two different reactions is excellent.

The level density is closely connected to the entropy S of the system at a given excitation energy E_x . This opens the possibility of investigating certain thermodynamic properties in the atomic nucleus. The entropy is given by

$$S(E_x) = k_B \ln \Omega(E_x). \quad (5)$$

The Boltzmann's constant k_B is set to unity from here on. The multiplicity Ω is directly proportional to the level density: $\Omega(E_x) = \rho(E_x)/\rho_0$. The ground states of

even-even nuclei represents a well-ordered system with no thermal excitations and are characterized by zero entropy and temperature. Therefore the normalization denominator is set to $\rho_0 = 3$ MeV⁻¹ to obtain $S = \ln \Omega \sim 0$ in the ground state band region. This ensures that the ground band properties fulfill the third law of thermodynamics with $S(T \rightarrow 0) = 0$. The extracted ρ_0 is also used for the odd-mass neighboring nuclei.

Figure 3 shows the entropies S of ^{170,171,172}Yb obtained from the (³He, $\alpha\gamma$) reaction. Several properties derived from this figure are actually connected to the fact that these mid-shell rare earth nuclei have similar nuclear structure and global properties, such as nuclear deformation.

The entropies (or level densities) of ¹⁷⁰Yb and ¹⁷²Yb follow each other closely as a function of excitation energy. In particular, in the excitation energy region from the ground state up to 2 MeV, $S(E_x)$ shows very similar shapes. We interpret the strong increase around 1.5 MeV of excitation energy as the breaking of the first Cooper pair. The next increase, which is much more smeared out, terminates near 2.5 MeV and reveals the beginning of the four quasiparticle regime. Above 2.5 MeV the entropy increases linearly [23].

In addition, all three entropy curves are parallel for excitation energies above $E_x \sim 2.5$ MeV. In the microcanonical ensemble, the slope of $S(E_x)$ is connected to the temperature by

$$T = (dS/dE_x)_V^{-1}. \quad (6)$$

A constant temperature least-square fit in the $E_x = 2.5 - 5.5$ MeV region of ^{170,171,172}Yb gives $T = 0.62(3), 0.52(4)$ and $0.58(3)$ MeV, respectively. These temperatures are interpreted as the critical temperatures T_c for the breaking of nucleon pairs.

It is interesting to note that the entropy of ¹⁷¹Yb shows a strongly increasing behavior that also terminates at $E_x \sim 1.5$ MeV revealing the first breaking of Cooper pairs in the underlying even-even core. Here the odd valence nucleon behaves as a passive spectator, however, the increase in $S(E_x)$ appears at slightly lower excitation energies than for the even systems. This behavior is attributed to the reduced pairing gap Δ resulting from the Pauli blocking by the valence neutron in the odd system.

The entropy carried by the valence neutron particle (or hole) can be estimated assuming that the entropy is an extensive (additive) quantity [24]. Figure 4 shows the observed single particle and hole entropies defined by

$$\Delta S(\text{particle}) = S(^{171}\text{Yb}) - S(^{170}\text{Yb}), \quad (7)$$

$$\Delta S(\text{hole}) = S(^{171}\text{Yb}) - S(^{172}\text{Yb}), \quad (8)$$

respectively. The single particle (or hole) carries about $\Delta S = 2$. Deviations from this estimate appear at low excitation energies due to the lower pairing gap in the odd-mass system. At higher energies the slightly lower critical temperature in the odd-mass system is responsible for the increasing entropy difference as function of

excitation energy. These two qualitative explanations are connected. The pairing gap Δ , critical temperature T_c and single particle (hole) entropy ΔS are related [24] by

$$T_c = \frac{1}{\Delta S} \Delta, \quad (9)$$

for constant ΔS . This is consistent with the present observations. Thus, it is reasonable to expect that if both Δ and T_c were equal in the systems compared, the ΔS curve would be flatter as function of excitation energy.

The thermodynamical properties can also be studied using the canonical ensemble. Recently [25] this was performed for the $^{160,161,162}\text{Dy}$ isotopes that behave very much in the same way as the present Yb isotopes.

IV. GAMMA-RAY STRENGTH FUNCTIONS

The γ -ray transmission coefficient $\mathcal{T}(E_\gamma)$ in Eq. (1) is expressed as a sum of all the γ -ray strength functions f_{XL} of multiplicities XL

$$\mathcal{T}(E_\gamma) = 2\pi \sum_{XL} E_\gamma^{2L+1} f_{XL}(E_\gamma). \quad (10)$$

The radiative transmission coefficient \mathcal{T} obtained from the present work is unnormalized. As shown in Eqs. (2,3) and in the previous section, two of the three normalization coefficients are obtained from the level density. The remaining constant B in Eq. (3) is determined using information from neutron resonance decay. The average radiative width of neutron resonances $\langle \Gamma_\gamma \rangle$ at the neutron binding energy is related to $\mathcal{T}(E_\gamma)$

$$\langle \Gamma_\gamma \rangle = \frac{B}{4\pi\rho(B_n, J_i^\pi)} \sum_{J_f^\pi} \int_0^{B_n} dE_\gamma \mathcal{T}(E_\gamma) \rho(B_n - E_\gamma, J_f^\pi), \quad (11)$$

where $D_i = 1/\rho(B_n, J_i^\pi)$ is the average spacing of s -wave neutron resonances, and the sum extends over all possible final state spins and parities, and matching multipole contribution to $\mathcal{T}(E_\gamma)$. The level density is assumed to have the standard energy and spin dependent parts

$$\rho(E_x, J) = \rho(E_x) \frac{2J+1}{2\sigma^2} e^{-(J+1/2)^2/2\sigma^2}, \quad (12)$$

where σ is the spin cut-off parameter, and we assume equal number of positive and negative parity states. The spin cut-off parameter is calculated as a function of excitation energy by a linearization of the usual $\sigma \sim U^{1/4}$ around B_n

$$\sigma = \sigma_0 \left(1 + \frac{E_x - B_n}{4(B_n - \Delta)} \right), \quad (13)$$

where σ_0 is the spin cut-off parameter at the neutron binding energy calculated according to [1], and the pairing parameter Δ is the same as in Eq. (4). This formula

has the advantage that $\sigma(E_x)$ remains finite for all excitation energies and therefore one is not forced to make additional assumptions for σ below Δ . A detailed description of the calculation of the integral in Eq. (11), including the necessary extrapolation of experimental data to cover the energy region under consideration, is given in [10]. The normalized experimental radiative strength functions for $^{170,171,172}\text{Yb}$ are shown in Figure 5.

It is assumed that the radiative strength is dominated by dipole transitions. The Kadmenskiĭ-Markushev-Furman (KMF) model is employed for the $E1$ strength. In the KMF model [17], the Lorentzian GEDR is modified in order to reproduce the non-zero limit of the GEDR for $E_\gamma \rightarrow 0$ by means of a temperature-dependent width of the GEDR. The $E1$ strength in the KMF model is given by

$$f_{E1}(E_\gamma) = \frac{1}{3\pi^2 \hbar^2 c^2} \frac{0.7\sigma_{E1}\Gamma_{E1}^2(E_\gamma^2 + 4\pi^2 T^2)}{E_{E1}(E_\gamma^2 - E_{E1}^2)^2}, \quad (14)$$

where σ_{E1} , Γ_{E1} , and E_{E1} are the cross section, width, and the centroid of the GEDR determined from photoabsorption experiments. We adopt the KMF model with the temperature T taken as a constant to be consistent with our assumption that the radiative strength function is independent of excitation energy. The width of the GEDR is a sum of energy and temperature dependent parts

$$\Gamma_{E1}(E_\gamma, T) = \frac{\Gamma_{E1}}{E_{E1}^2} (E_\gamma^2 + 4\pi^2 T^2). \quad (15)$$

The giant dipole resonance is split into two parts for deformed nuclei. Therefore, a sum of two strength functions each described by the above equations is used.

For the $M1$ radiation f_{M1} , the Lorentzian giant magnetic dipole resonance (GMDR)

$$f_{M1}(E_\gamma) = \frac{1}{3\pi^2 \hbar^2 c^2} \frac{\sigma_{M1} E_\gamma \Gamma_{M1}^2}{(E_\gamma^2 - E_{M1}^2)^2 + E_\gamma^2 \Gamma_{M1}^2}, \quad (16)$$

is adopted. This corresponds to a spin-flip excitation.

A contribution from $E2$ radiation is not included in Eq. (11) because its strength is much smaller than the uncertainty due to the integration. The Lorentzian $E2$ radiative strength

$$f_{E2}(E_\gamma) = \frac{1}{5\pi^2 \hbar^2 c^2 E_\gamma^2} \frac{\sigma_{E2} E_\gamma \Gamma_{E2}^2}{(E_\gamma^2 - E_{E2}^2)^2 + E_\gamma^2 \Gamma_{E2}^2}, \quad (17)$$

is included in the summed radiative strength function for completeness.

For several rare-earth nuclei, an anomalous resonance structure is observed in the radiative strength function [10,25]. This resonance is observed in all rare-earth nuclei that have been investigated by the Oslo method and

is referred to as a pygmy resonance. In order to reproduce experimental results where the pygmy resonance is observed, another Lorentzian centered at E_{py} with width Γ_{py} and cross section σ_{py} is used in addition to the GEDR, GMDR, and the $E2$ resonance described above. The total radiative strength function is composed of four parts

$$f(E_\gamma) = \kappa(f_{E1}^{I,II} + f_{M1}) + E_\gamma^2 f_{E2} + f_{py}, \quad (18)$$

where $f_{E1}^{I,II}$ has the two components of the GEDR given by the KMF model Eq. (14), f_{M1} and f_{E2} are the giant magnetic dipole and electric quadrupole resonances given by Eqs. (16) and (17), respectively. The parameters of these resonances are taken from [20] and are listed in Table I. The parameters for the pygmy resonance f_{py} and the overall multiplicative constant κ were treated as fitting parameters, as well as the T -parameter of the KMF model.

The values obtained from the fit are listed in Table II. The overall normalization factor κ should be close to 1. The deviation from 1 may be due to the normalization of the radiative strength function by the total radiative width or the approximation in the factor 0.7 in the KMF model. The energy and width of the pygmy resonance in $^{171,172}\text{Yb}$ from the different experiments agree well.

In Figure 6, a fit to the experimental radiative strength function is shown. The upper panels contain the total radiative strength function (RSF) and the lower panels show the contribution from the pygmy resonance. After subtracting the fit function without the pygmy resonances (dashed lines) from the data points of the upper panel, the pygmy resonance is clearly identified. The fit using only the pygmy resonances is shown as solid lines in the lower panels.

The RSFs from the ($^3\text{He}, \alpha\gamma$) reactions are similar. The pygmy resonances seem to be split into two components. The two-bump structure is so pronounced in ^{170}Yb that a fit with κ and T as free parameters failed. Therefore, the corresponding resonance parameters could not be listed in Table II. We fixed the T parameter from values for other Yb isotopes to be 0.34. A similar splitting has been observed for Dy isotopes [23], although the fits with one component usually give satisfying results, e.g. for the case of ^{172}Yb , both the one- and two-component fits give reasonable descriptions of the data. Examples of two-component fits to the residual RSF (after subtracting contributions from giant resonances) are shown in Figure 7, the corresponding resonance parameters are given in Table III. By inspection of Figure 6, a very weak structure at $E_\gamma \sim 2.1$ MeV seems to be apparent in ^{171}Yb as well.

In the case of ^{172}Yb , the multipolarity of the pygmy resonance has been established to be $M1$ [26]. The resonance parameters are in reasonable agreement with theory [27] and nuclear resonance fluorescence (NRF) experiments [28] if we assume that for the scissors mode in the quasicontinuum (above the pairing gap), the mo-

ment of inertia is close to the rigid-body value and bare g factors have to be applied. NRF experiments on Dy isotopes show that $M1$ excitations cluster around ~ 2.4 and ~ 3.0 MeV [29]. In the present work, the splitting into two components of the pygmy resonance could be explained tentatively by the splitting in energy of $\Delta K = \pm 1$ $M1$ γ rays in the quasicontinuum.

V. CONCLUSIONS

The level densities and radiative strength functions in ^{170}Yb and ^{171}Yb are obtained from measured γ -ray spectra following ^3He induced reaction on ^{171}Yb . The deduced level densities extend structure data to excitation energies above ~ 2 MeV where the tabulated levels are incomplete. The level densities and entropies for ^{170}Yb and ^{172}Yb follow each other closely as a function of excitation energy. The step structures in the level density indicate the breaking of the nucleon Cooper pair. The entropy carried by the valence neutron particle (or hole) in ^{171}Yb is estimated to be $\Delta S = 2k_B$ as expected. The radiative strength function in ^{171}Yb exhibits a resonance structure (pygmy resonance) similar to that observed in a previous measurement. The parameters for the pygmy resonance were obtained by fitting the radiative strength function with common models, and compared to values from the $^{172}\text{Yb}(^3\text{He}, \alpha)^{171}\text{Yb}$ reaction. There is a good agreement between the two measurements. The level density and strength function in ^{171}Yb and ^{172}Yb using two different reactions give essentially the same results leading to increased confidence to the applicability of statistical γ -ray spectroscopy.

ACKNOWLEDGMENTS

This research was sponsored by the National Nuclear Security Administration under the Stewardship Science Academic Alliances program through DOE Research Grant No. DE-FG03-03-NA00076. Support by U.S. Department of Energy Grant No. DE-FG02-97-ER41042 is acknowledged. Part of this work was performed under the auspices of the U.S. Department of Energy by the University of California, Lawrence Livermore National Laboratory under Contract No. W-7405-ENG-48. Financial support from the Norwegian Research Council (NFR) is acknowledged.

-
- [1] A. Gilbert and A.G.W. Cameron, Can. J. Phys. **43**, 1446 (1965).
 - [2] T. von Egidy, H. H. Schmidt, and A.N. Behkami, Nucl. Phys. **A481**, 189 (1988).

- [3] Samuel S. Dietrich and Barry L. Berman, *At. Data Nucl. Data Tables* **38**, 199 (1988).
- [4] J. Kopecky and M. Uhl, *Phys. Rev. C* **41**, 1941 (1990).
- [5] A. Schiller, L. Bergholt, M. Guttormsen, E. Melby, J. Rekstad, and S. Siem, *Nucl. Instrum. Methods Phys. Res. A* **447**, 498 (2000).
- [6] L. Henden, L. Bergholt, M. Guttormsen, J. Rekstad, and T.S. Tveter, *Nucl. Phys.* **A589**, 249 (1995).
- [7] E. Tavukcu, Ph.D. thesis, North Carolina State University, 2002; A. Schiller *et al.*, *Phys. Rev. C* **68**, 054326 (2003).
- [8] M. Guttormsen, E. Melby, J. Rekstad, S. Siem, A. Schiller, T. Lönnroth, and A. Voinov, *J. Phys. G* **29**, 263 (2003).
- [9] A. Schiller, A. Bjerve, M. Guttormsen, M. Hjorth-Jensen, F. Ingebretsen, E. Melby, S. Messelt, J. Rekstad, S. Siem, and S.W. Ødegård, *Phys. Rev. C* **63**, 021306(R) (2001).
- [10] A. Voinov, M. Guttormsen, E. Melby, J. Rekstad, A. Schiller, and S. Siem, *Phys. Rev. C* **63**, 044313 (2001).
- [11] A. Schiller, Ph.D. thesis, University of Oslo, 2000.
- [12] M. Guttormsen, A. Atac, G. Løvholden, S. Messelt, T. Ramsøy, J. Rekstad, T.F. Thorsteinsen, T.S. Tveter, Z. Zelazny, *Phys. Scr.* **T32**, 54 (1990).
- [13] M. Guttormsen, T.S. Tveter, L. Bergholt, F. Ingebretsen, J. Rekstad, *Nucl. Instrum. Methods Phys. Res. A* **374**, 371 (1996).
- [14] M. Guttormsen, T. Ramsøy, and J. Rekstad, *Nucl. Instrum. Methods Phys. Res. A* **255**, 518 (1987).
- [15] D.M. Brink, Ph.D. thesis, Oxford University, 1955.
- [16] P. Axel, *Phys. Rev.* **126**, 671 (1962).
- [17] S.G. Kadomenskiĭ, V.P. Markushev, and V.I. Furman, *Yad. Fiz.* **37**, 277 (1983), [*Sov. J. Nucl. Phys.* **37**, 165 (1983)].
- [18] G. Gervais, M. Thoennessen, and W. E. Ormand, *Phys. Rev. C* **58**, R1377 (1998).
- [19] R. Firestone and V.S. Shirley, Vol. II, *Table of Isotopes, 8th edition* (Wiley, New York, 1996).
- [20] Handbook for Calculations of Nuclear Reactions Data, IAEA, Vienna, Report No. IAEA-TECDOC-1024, 1998.
- [21] J. Dobaczewski, P. Magierski, W. Nazarewicz, W. Satuła, and Z. Szymański, *Phys. Rev. C* **63**, 024308 (2001).
- [22] A. Schiller, M. Guttormsen, E. Melby, J. Rekstad, and S. Siem, *Phys. Rev. C* **61**, 044324 (2000).
- [23] M. Guttormsen, R. Chankova, M. Hjorth-Jensen, J. Rekstad, S. Siem, A. Schiller, D. J. Dean, *Phys. Rev. C* **68**, 034311 (2003).
- [24] M. Guttormsen, M. Hjorth-Jensen, E. Melby, J. Rekstad, A. Schiller, and S. Siem, *Phys. Rev. C* **63**, 044301 (2001).
- [25] M. Guttormsen, A. Bagheri, R. Chankova, J. Rekstad, S. Siem, A. Schiller, and A. Voinov, *Phys. Rev. C* **68**, 064306 (2003).
- [26] A. Schiller, A. Voinov, E. Algin, J. A. Becker, L. A. Bernstein, P. E. Garrett, M. Guttormsen, R. O. Nelson, J. Rekstad, S. Siem, *nucl-ex/0401038*.
- [27] E. Lipparini, S. Stringari, *Phys. Lett.* **130B**, 139 (1983).
- [28] A. Zilges, P. von Brentano, C. Wesselborg, R. D. Heil, U. Kneissl, S. Lindenstruth, H. H. Pitz, U. Seemann, R. Stock, *Nucl. Phys.* **A507**, 399 (1990); **A519**, 848 (1990).
- [29] J. Margraf *et al.*, *Phys. Rev. C* **52**, 2429 (1995).

TABLE I. Parameters used in the fits to the radiative strength functions.

	^{170}Yb	^{171}Yb	^{172}Yb
E_{E1}^I , MeV	12.05	12.25	12.25
σ_{E1}^I , mb	239	239	239
Γ_{E1}^I , MeV	2.78	2.6	2.6
E_{E1}^{II} , MeV	15.38	15.5	15.5
σ_{E1}^{II} , mb	302	302	302
Γ_{E1}^{II} , MeV	4.64	4.8	4.8
E_{M1} , MeV	7.4	7.5	7.5
σ_{M1} , mb	1.30	1.50	1.76
Γ_{M1} , MeV	4	4	4
E_{E2} , MeV	11.37	11.35	11.33
σ_{E2} , mb	6.75	6.77	6.80
Γ_{E2} , MeV	4.07	4.06	4.05
$\langle \Gamma_\gamma \rangle$, meV	80(20)	63(10)	75(10)

TABLE II. Fitted pygmy resonance parameters and normalization constants.

Reaction	E_{py} (MeV)	σ_{py} (mb)	Γ_{py} (MeV)	T (MeV)	κ
$^{171}\text{Yb}(^3\text{He}, ^3\text{He}')^{171}\text{Yb}$	3.54(10)	0.50(09)	0.91(18)	0.31(2)	1.26(06)
$^{172}\text{Yb}(^3\text{He}, \alpha)^{171}\text{Yb}$	3.35(19)	0.58(20)	0.95(31)	0.34(6)	1.01(13)
$^{172}\text{Yb}(^3\text{He}, ^3\text{He}')^{172}\text{Yb}$	3.28(18)	0.48(12)	1.36(41)	0.33(4)	1.65(11)
$^{173}\text{Yb}(^3\text{He}, \alpha)^{172}\text{Yb}$	3.38(27)	0.58(29)	0.99(55)	0.37(5)	1.85(17)

^a The RSF of ^{170}Yb could not be fitted by a single pygmy resonance, see text.

TABLE III. Parameters for the two-component pygmy resonances

Reaction	Component	E_{py} (MeV)	σ_{py} (mb)	Γ_{py} (MeV)
$^{171}\text{Yb}(^3\text{He}, \alpha)^{170}\text{Yb}$	I	2.15(21)	0.14(4)	1.23(53)
$^{171}\text{Yb}(^3\text{He}, \alpha)^{170}\text{Yb}$	II	3.38(10)	0.41(7)	1.13(50)
$^{173}\text{Yb}(^3\text{He}, \alpha)^{172}\text{Yb}$	I	2.56(16)	0.12(4)	0.72(34)
$^{173}\text{Yb}(^3\text{He}, \alpha)^{172}\text{Yb}$	II	3.41(4)	0.68(9)	0.60(13)

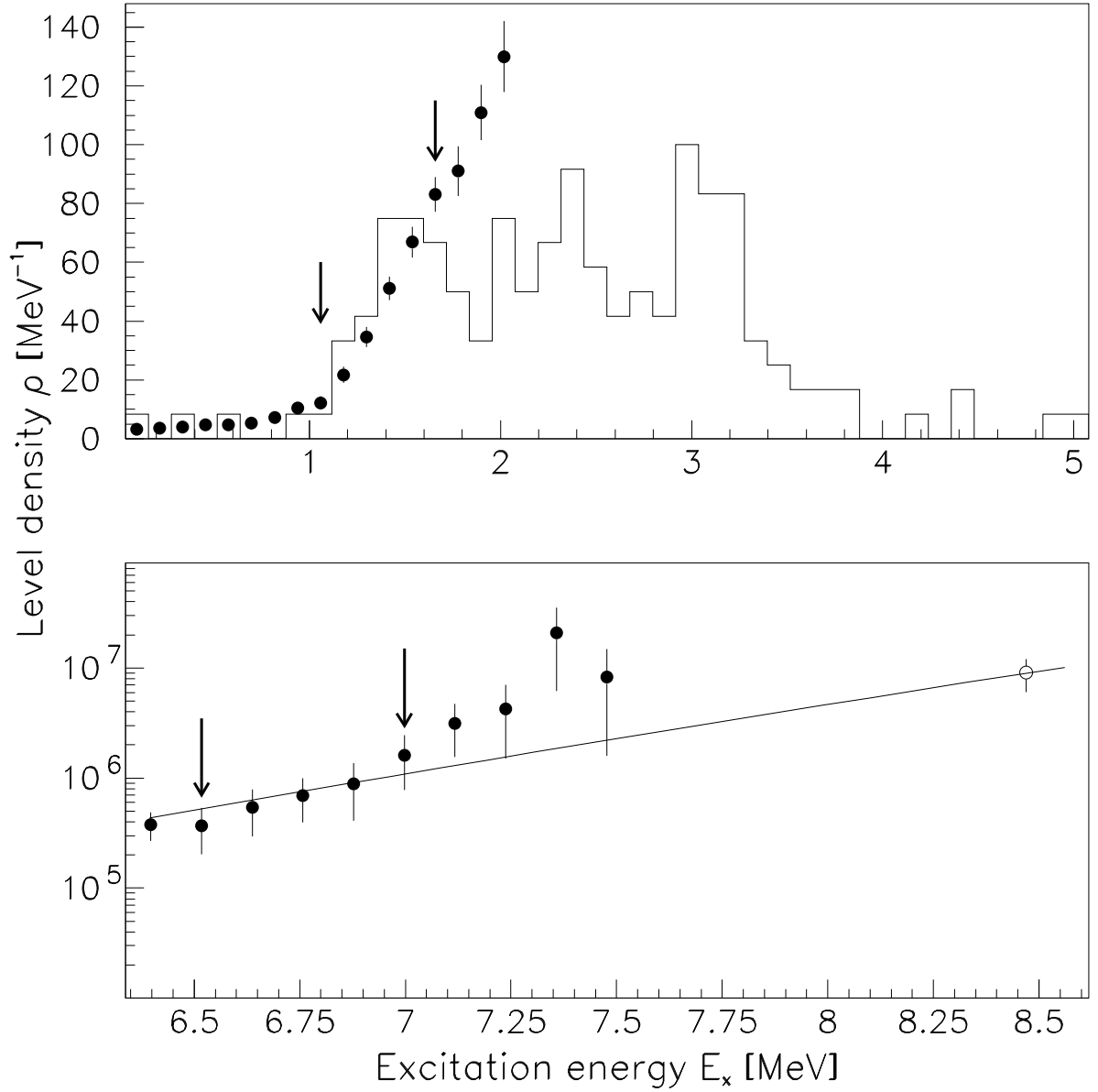


FIG. 1. Normalization procedure for the experimental ^{170}Yb level density. The experimental data from this paper are represented by full circles. In both panels, arrows enclose the data points used for normalization. The data were fit to discrete levels (shown as histograms in the upper panel) and to the level density calculated using the resonance spacings (shown as an open circle in the lower panel). The Fermi gas level density, Eq. 4, (line) was employed to connect the regions where data were available.

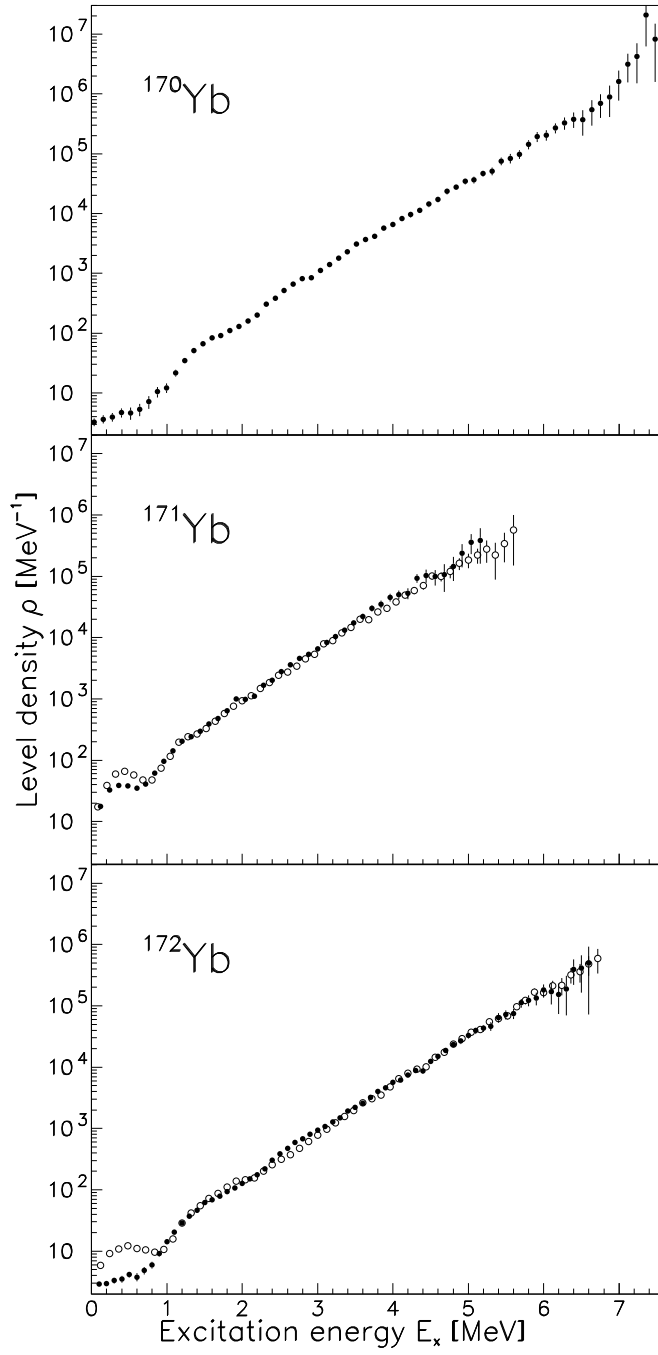


FIG. 2. Deduced level densities for $^{170,171,172}\text{Yb}$. The full and open circles correspond to data obtained from the $(^3\text{He}, \alpha)$ and $(^3\text{He}, ^3\text{He}')$ reactions, respectively.

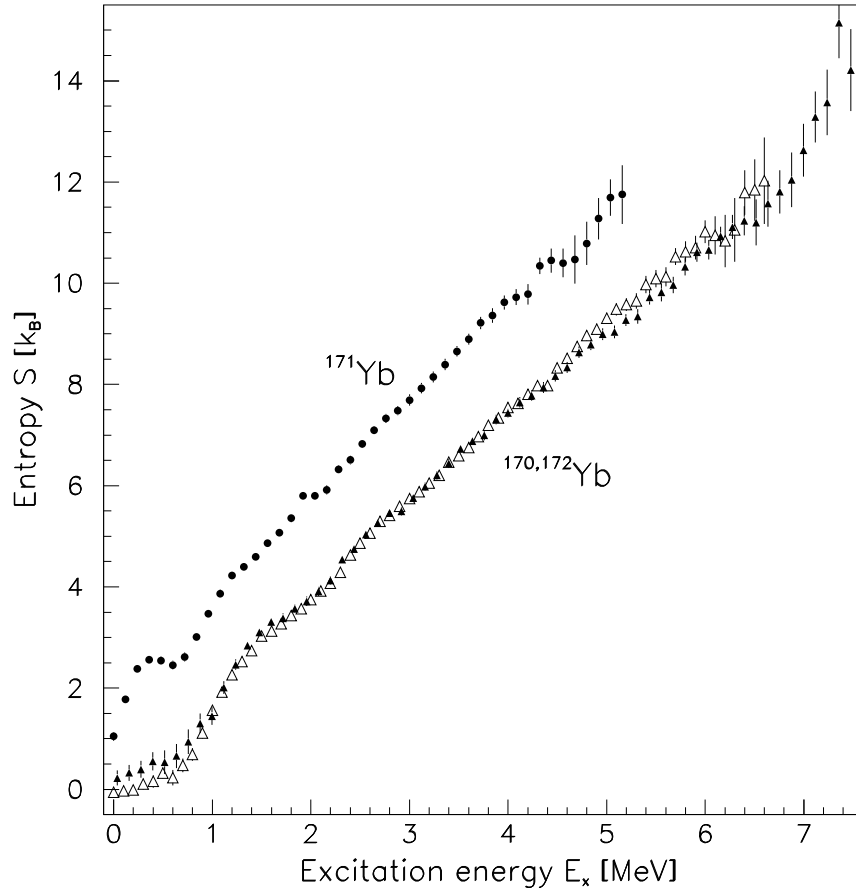


FIG. 3. Deduced entropies for $^{170,171,172}\text{Yb}$. All data are from the $(^3\text{He},\alpha)$ reaction. The full circles correspond to ^{171}Yb . The full and open triangles correspond to ^{170}Yb and ^{172}Yb , respectively.

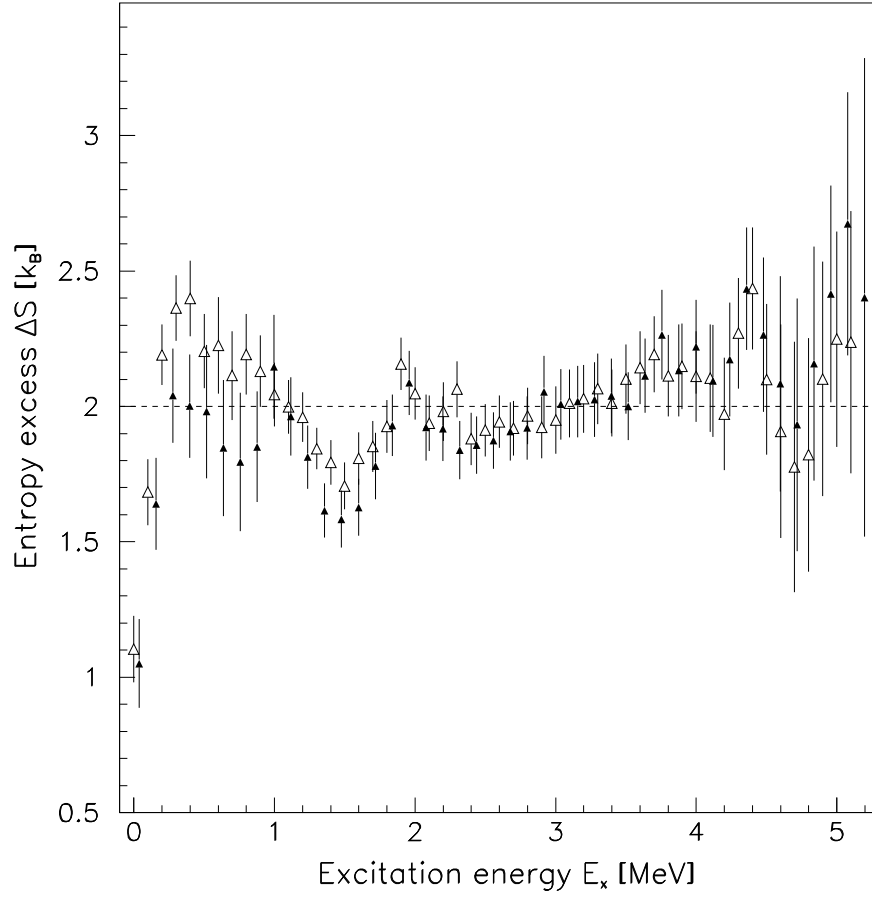


FIG. 4. Deduced entropy excess for ^{171}Yb . The full and open triangles correspond to entropy excesses for the single particle and hole, respectively, calculated using Eqs. (7) and (8). The entropy excess $\Delta S = 2k_B$ is shown by the dashed line.

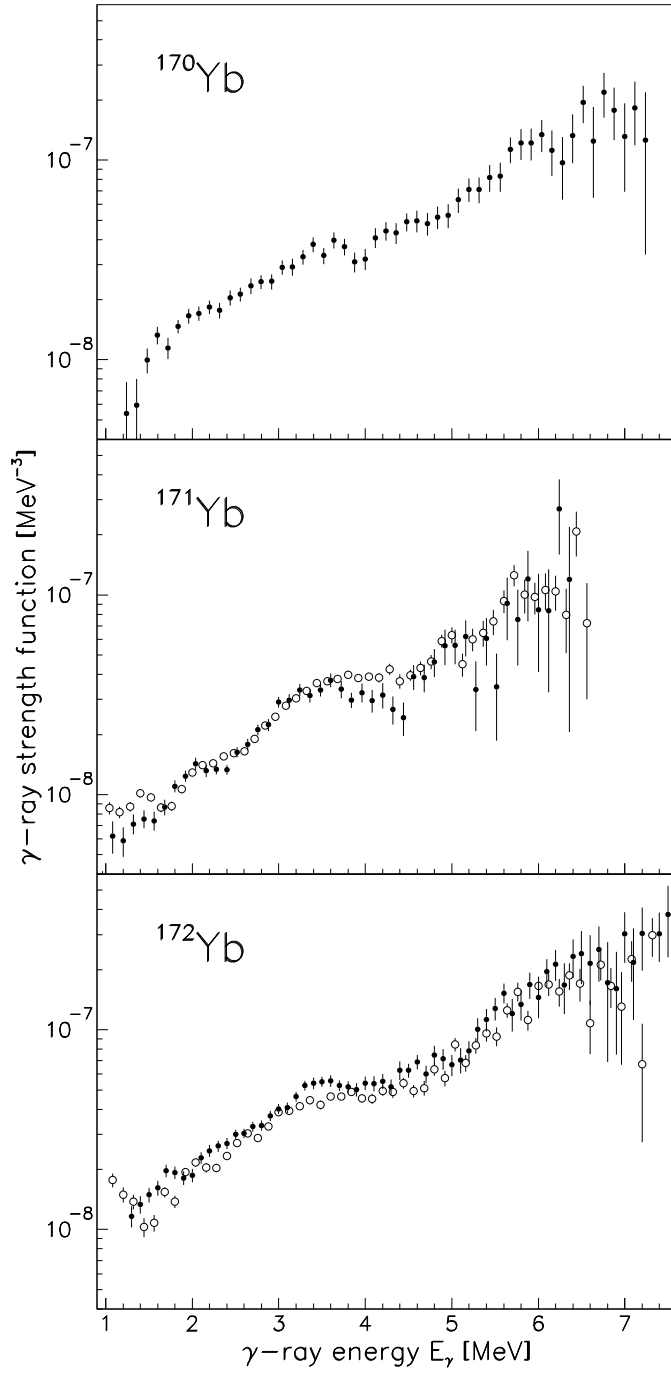


FIG. 5. Radiative strength functions for $^{170,171,172}\text{Yb}$. The full and open circles correspond to data obtained from the $(^3\text{He},\alpha)$ and $(^3\text{He},^3\text{He}')$ reactions, respectively.

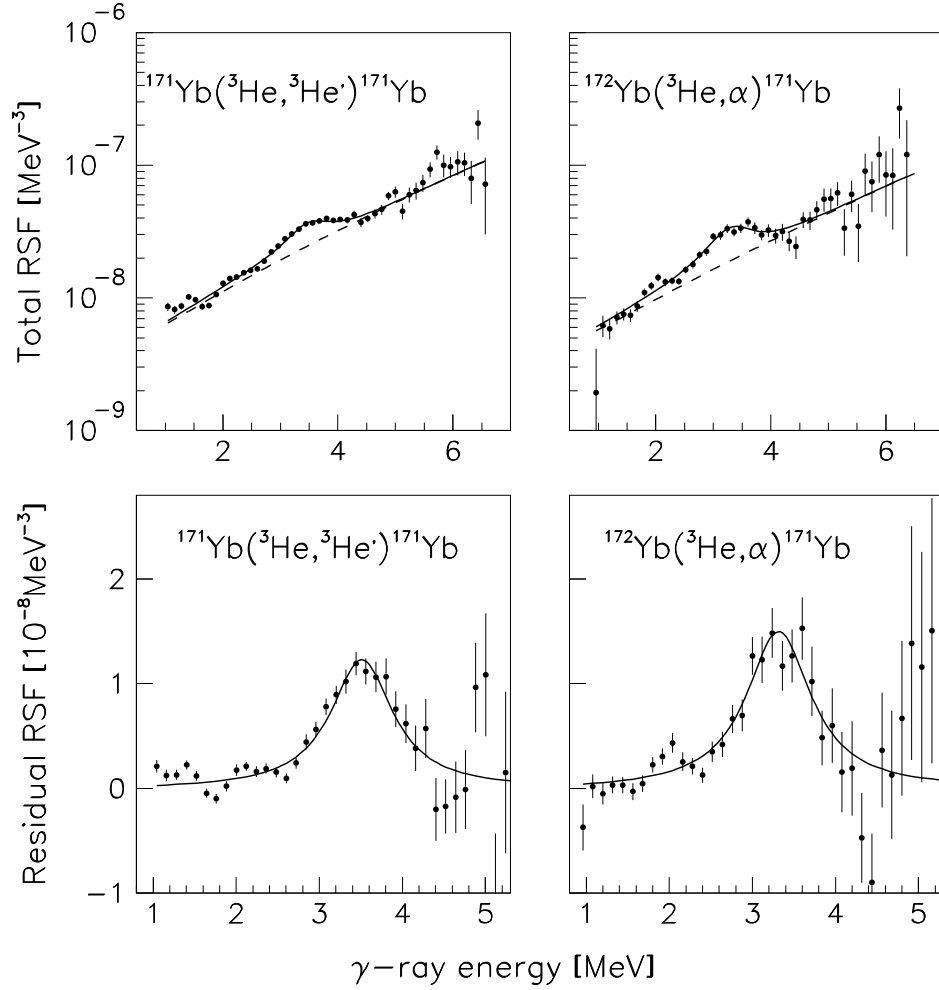


FIG. 6. A pygmy resonance in ^{171}Yb observed in two reactions. The left two panels correspond to data obtained from the $({}^3\text{He}, {}^3\text{He}')$ reaction. The two right panels show data from the $({}^3\text{He}, \alpha)$ reaction. The solid line in the upper panels is a fit to data including all contributions, the dashed lines are fits with the contribution from the pygmy resonance removed. The difference between the total γ -ray strength function data and the fit without the pygmy resonance (labeled as residual RSF) is shown in the lower panels. The pygmy resonance is clearly identified.

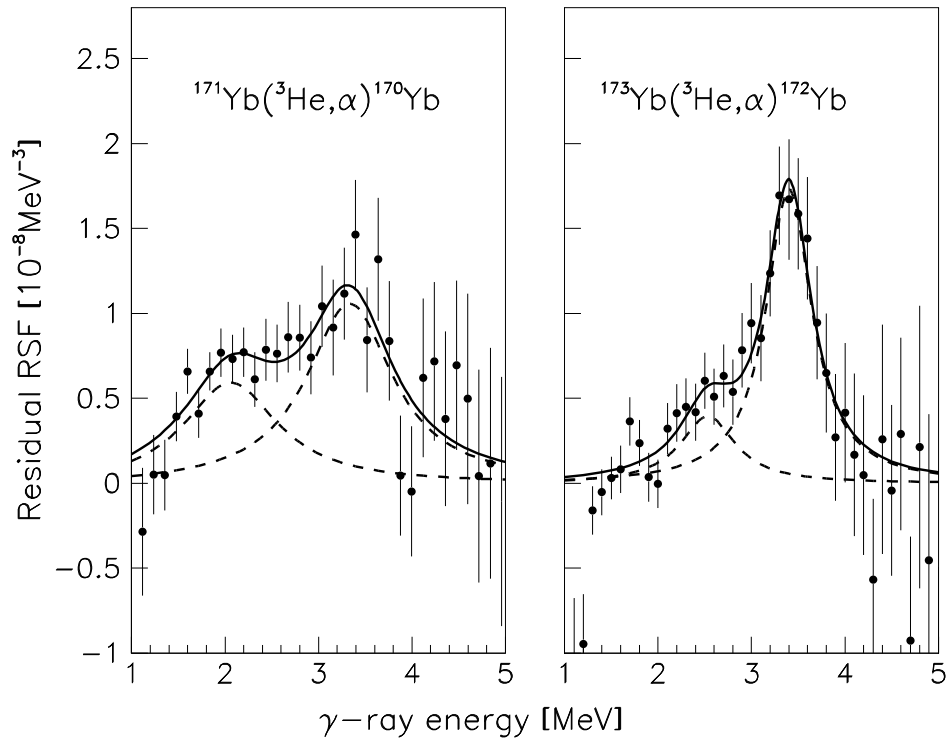


FIG. 7. Two component fits of the pygmy resonances in $^{170,172}\text{Yb}$. The total fit (solid line) is described by the sum of two pygmy resonances (dashed lines).